


RESEARCH ARTICLE

Open Access



gem-Difluorobisarylic derivatives: design, synthesis and anti-inflammatory effect

Abeer J. Ayoub^{1,2†}, Layal Hariss^{3†}, Nehme El-Hachem^{4,8†}, Ghewa A. El-Achkar¹, Sandra E. Ghayad⁵, Oula K. Dagher¹, Nada Borghol², René Grée⁶, Bassam Badran², Ali Hachem^{3†}, Eva Hamade^{2†} and Aida Habib^{1,7*†} 

Abstract

Introduction: New fluorinated diaryl ethers and bisarylic ketones were designed and evaluated for their anti-inflammatory effects in primary macrophages.

Methods: The synthesis of the designed molecules started from easily accessible and versatile *gem*-difluoro propargylic derivatives. The desired aromatic systems were obtained using Diels–Alder/aromatization sequences and this was followed by Pd-catalyzed coupling reactions and, when required, final functionalization steps. Both direct inhibitory effects on cyclooxygenase-1 or -2 activities, protein expression of cyclooxygenase-2 and nitric oxide synthase-II and the production of prostaglandin E₂, the pro-inflammatory nitric oxide and interleukin-6 were evaluated in primary murine bone marrow-derived macrophages in response to lipopolysaccharide. Docking of the designed molecules in cyclooxygenase-1 or -2 was performed.

Results: Only fluorinated compounds exerted anti-inflammatory activities by lowering the secretion of interleukin-6, nitric oxide, and prostaglandin E₂, and decreasing the protein expression of inducible nitric oxide synthase and cyclooxygenase-2 in mouse primary macrophages exposed to lipopolysaccharide, as well as cyclooxygenase activity for some inhibitors with different efficiencies depending on the R-groups. Docking observation suggested an inhibitory role of cyclooxygenase-1 or -2 for compounds **A3**, **A4** and **A5** in addition to their capacity to inhibit nitrite, interleukin-6, and nitric oxide synthase-II and cyclooxygenase-2 expression.

Conclusion: The new fluorinated diaryl ethers and bisarylic ketones have anti-inflammatory effects in macrophages. These fluorinated compounds have improved potential anti-inflammatory properties due to the fluorine residues in the bioactive molecules.

Keywords: Fluorine, Diaryl ethers, Macrophages, Cyclooxygenase, Inflammation

Introduction

Diaryl ethers are key scaffolds present in many natural or synthetic organic molecules, which are often used in medicinal chemistry [1]. Fenoprofen for instance is one of the synthetic diarylethers [2] with nonsteroidal

anti-inflammatory, analgesic and antirheumatic effects [3]. More precisely, it is a derivative of 2-aryl propanoic acids, which is an important class of nonsteroidal anti-inflammatory drugs including flurbiprofen, ibuprofen, naproxen and fenoprofen.

Moreover, benzophenone analogues, such as ketoprofen, recently have been reported also as potent anti-inflammatory agents by inhibiting prostaglandin (PG) production [4, 5]. It has been shown that benzoylphenyl acetic acid for instance has anti-inflammatory activity by decreasing the volume of paw edema in treated rats [6].

On the other hand, the introduction of fluorine into organic molecules may cause profound pharmacological

*Correspondence: ah31@aub.edu.lb

†Abeer J. Ayoub, Layal Hariss and Nehme El-Hachem contributed equally to the work

†Ali Hachem, Eva Hamade and Aida Habib are senior authors and contributed equally to this work

¹ Department of Biochemistry and Molecular Genetics, Faculty of Medicine, American University of Beirut, Beirut, Lebanon

Full list of author information is available at the end of the article



effects by improving the activity and selectivity of the bioactive molecules [7]. The utility of fluorine in the design of drugs results mainly from its ability to modify some functional activities, such as increasing lipophilicity [8] and extending its bioavailability [9]. Moreover, carbon forms stronger bond with fluorine (CF)_n, with a higher oxidative and thermal stability than a carbon–hydrogen bond [10]. The CF₂ unit for instance is generally considered as a bioisostere of the oxygen atom or of a carbonyl group [11].

We therefore synthesized new *gem*-difluorobisarylic derivatives and evaluated their anti-inflammatory effects. We first investigated their effects on PGE₂ production in mouse primary macrophages in response to lipopolysaccharide (LPS) and their anti-cyclooxygenase (COX)-1 and -2 activities. We next studied their effects on the production of the pro-inflammatory nitric oxide (NO) and interleukin (IL)-6 and the expression of NO synthase-II (NOS-II) and COX-2.

Results and discussion

Synthesis of bisarylic derivatives

Based on our previous study [12], five bisarylic compounds **A1** to **A5** were designed as indicated in Scheme 1.

In our strategy, the *gem*-difluoro unit has been chosen as a mimic of either the ether oxygen (fenoprofen series) or of a carbonyl group (ketoprofen series). First, two phenylpropionic acid derivatives **A1** (as a non-fluorinated

reference) and the corresponding *gem*-difluoro derivative **A2** were proposed as analogues of fenoprofen and ketoprofen. The comparison of the inhibitory activities of compounds **A1** and **A2** would allow establishing the impact of fluorine atom on the efficiency of these compounds. On the other hand, three other derivatives **A3**, **A4**, and **A5** were designed as simplified benzoic acid-type derivatives, with three different substituents in *meta* position on the second aromatic ring (Scheme 1).

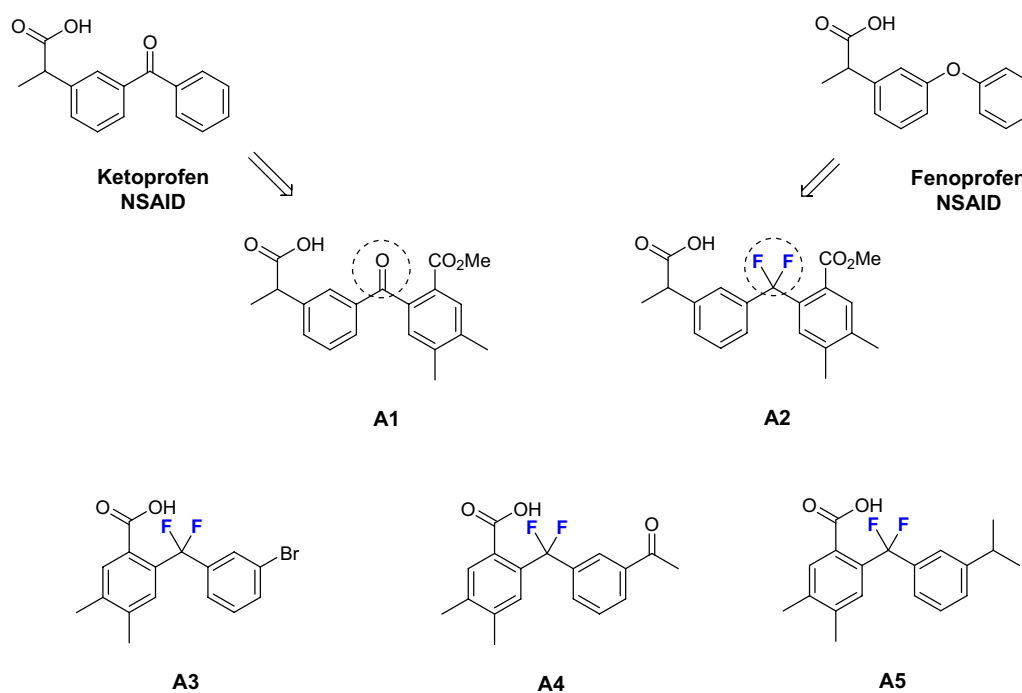
Synthetic procedures

All these molecules were synthesized from bromo intermediates **B** (Scheme 2, Table 1) and were tested for their anti-inflammatory activity.

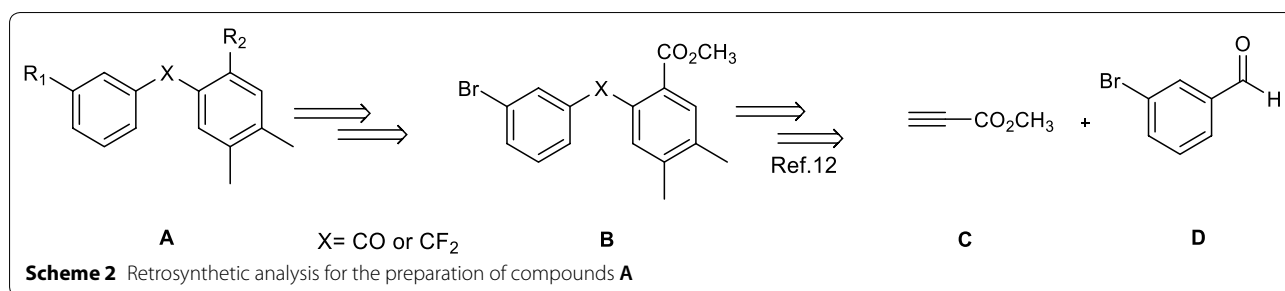
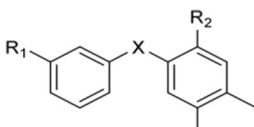
Synthesis of key intermediates **7** and **10**

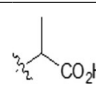
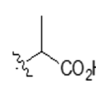
Addition of the lithium salt of compound **2** to 3-bromobenzaldehyde **3** at low temperature (−80 °C) gave propargyl alcohol **4** in 70% yield. After oxidation with Jones reagent, propargylic ketone **5** was isolated in 80% yield. Then, Diels–Alder reaction and DDQ aromatization provided the intermediate **7** with a good yield for both steps (Scheme 3).

After treatment of ketone **5** by DAST, compound **8** was obtained in 71% yield. Similarly, Diels–Alder reaction and DDQ aromatization proceeded well by giving the fluorinated intermediate **10** with excellent yields (Scheme 4).



Scheme 1 Design of target molecules

**Table 1** Preparation of five bisarylic compounds


Compound	X	R ₁	R ₂
A1	C=O		-CO ₂ CH ₃
A2	CF ₂		-CO ₂ CH ₃
A3	CF ₂	Br	-CO ₂ H
A4	CF ₂	-COCH ₃	-CO ₂ H
A5	CF ₂	-CH(CH ₃) ₂	-CO ₂ H

Preparation of compounds A1 and A2

Starting from the key scaffolds **7** and **10**, Suzuki–Miyaura couplings, with boronic acid, afforded biphenyl type compounds **11** and **12** in 92 and 94% yield, respectively.

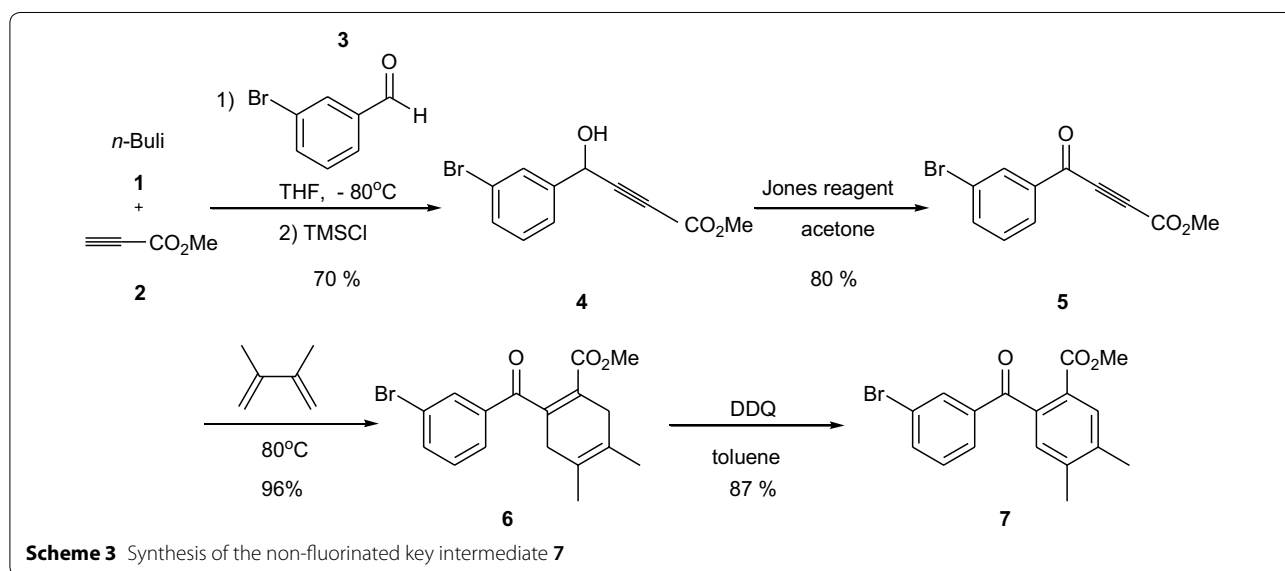
Then, hydroboration to **13** and **14**, followed by oxidation with Jones reagent led to the desired analogues **A1** and **A2** in good yields (Scheme 5).

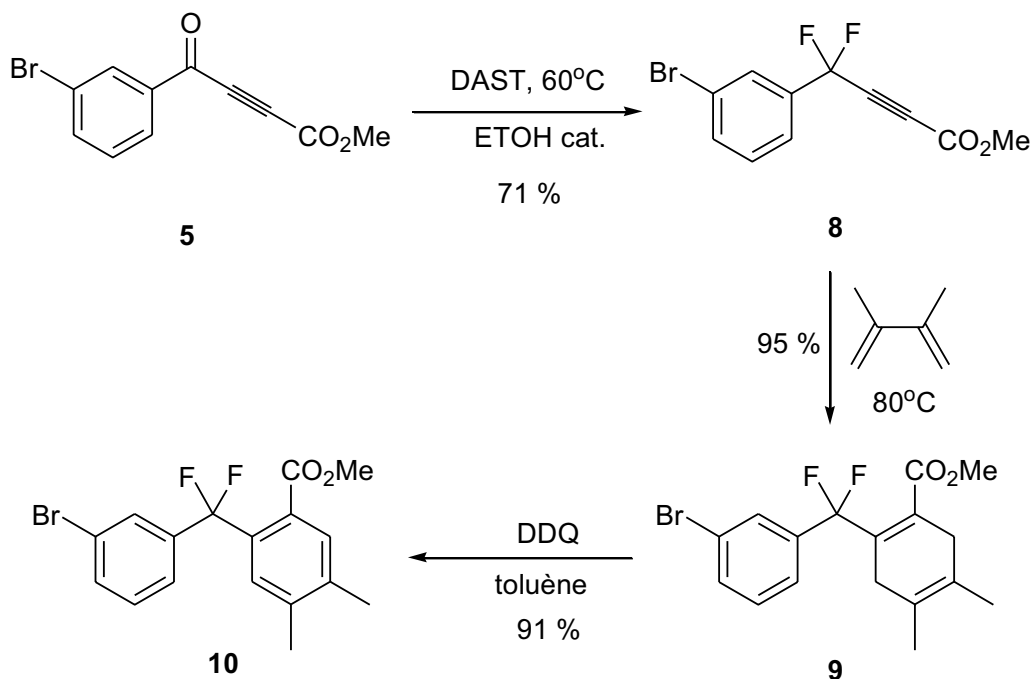
Preparation of compounds A3, A4, and A5

Starting from intermediates **10** and **12**, reduction with LiBEt₃H furnished alcohols **15** and **16** respectively, then oxidation by Jones reagent gave the desired acid **A3**. However, in the case of **16**, an unexpected cleavage of the double bond occurred, affording acid **A4**. Using the same *gem*-difluoro intermediate **12**, catalytic hydrogenation to **17**, followed by reduction and oxidation afforded the desired derivative **A5** in good yields (Scheme 6).

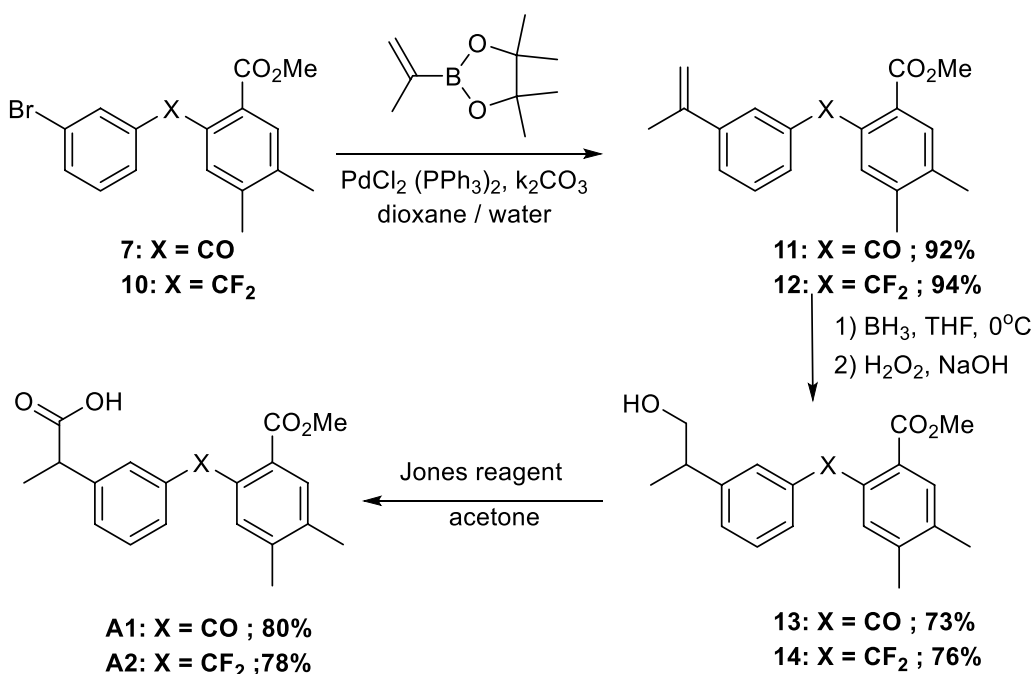
Biological activities

We investigated the effects of these derivatives on inflammation in bone marrow-derived macrophages (BMDM) by first evaluating their capacity to decrease LPS-dependent increase of PGE₂ secretion and COX-2 expression. Compound **A1** (non-fluorinated) and compound **A2** (fluorinated) effects were compared to evaluate the importance of the fluorine atom. Only compound **A2** inhibited significantly in a dose-dependent manner the





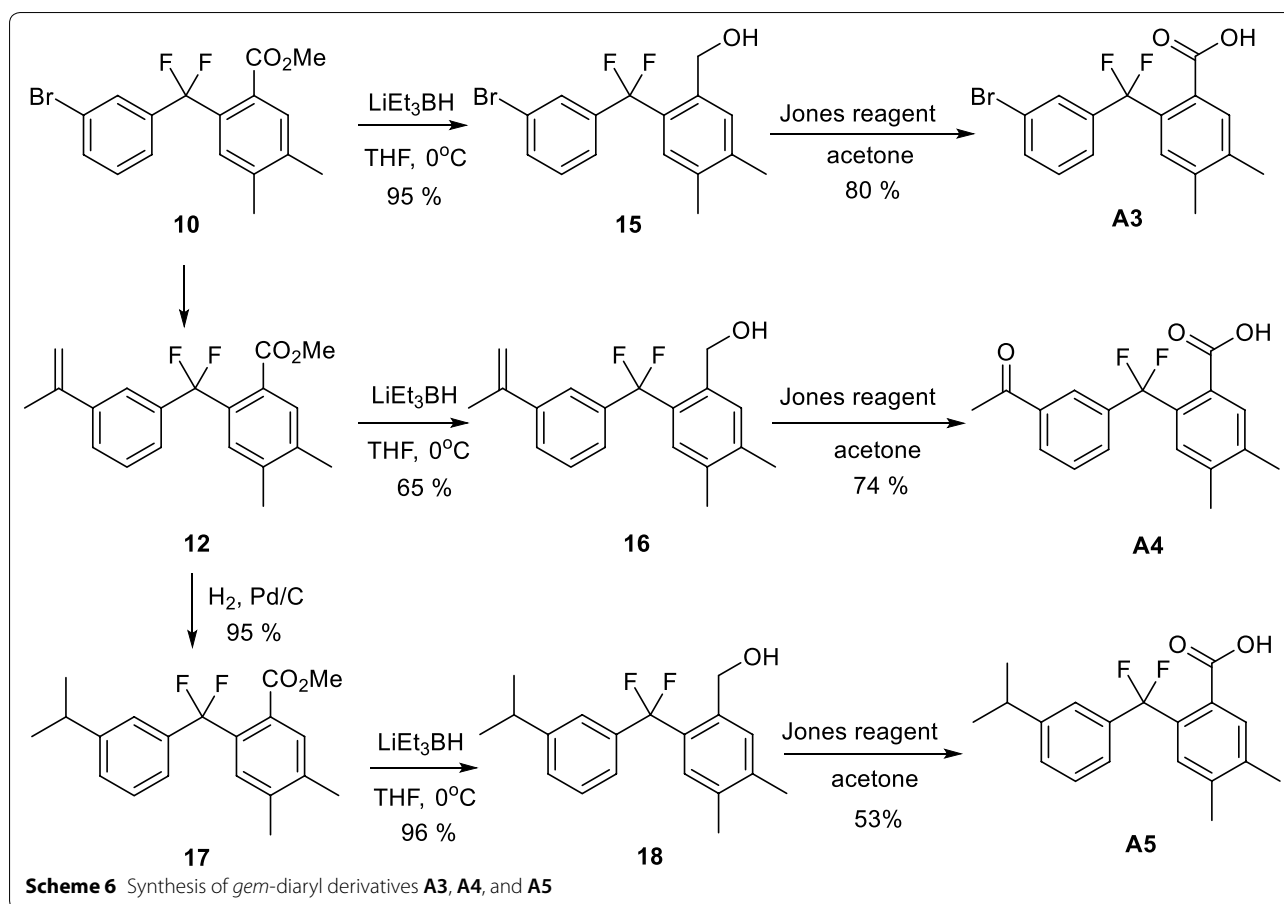
Scheme 4 Synthesis of the fluorinated key intermediate **10**



Scheme 5 Synthesis of derivatives **A1** and **A2**

secretion of PGE₂ (Fig. 1a) (IC₅₀ = 16.5 ± 8.9 μM) with no effect on COX-2 expression (Fig. 1c) supporting the importance of fluorine in inhibiting PGE₂ production.

In parallel, we compared the inhibitory effects of compounds **A3**, **A4** and **A5**, which are all fluorinated but present differences in R1 group (Table 1). Compound **A3** is



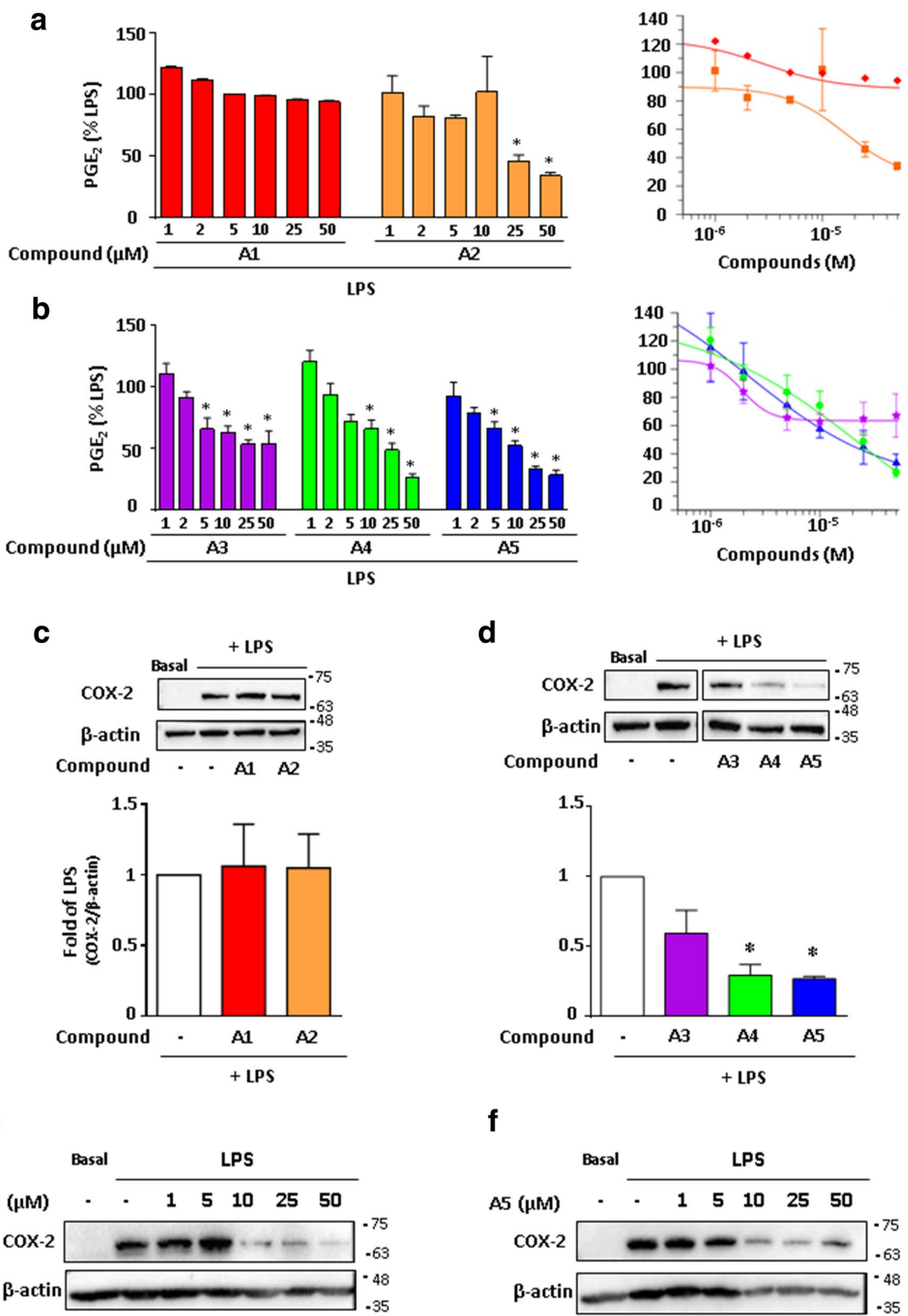
the bromine intermediate obtained in the synthetic reaction of compound **A5**. Compound **A4** is a ketone intermediate obtained unexpectedly with good yield during the synthesis of compound **A5**. Compounds **A3**, **A4** and **A5** have the carboxyl group attached to the benzene ring in the ortho position relative to CF_2 group.

Figure 1b showed a dose response effect of these derivatives on PGE_2 secretion, in which compounds **A4** and **A5** significantly decreased PGE_2 secretion at 25 and 50 μM with IC_{50} of 28.1 ± 22.8 and 22.4 ± 21.5 μM , respectively. Compound **A3** did not show a strong inhibition at similar concentrations. Under these conditions, only compounds **A4** and **A5** significantly downregulated COX-2 expression (Fig. 1d). Further analysis showed a dose-dependent

inhibitory effect on COX-2 expression for compounds **A4** and **A5** (Fig. 1e and f, respectively). Thus, the nature of R groups in compounds **A4** and **A5** is important for their inhibitory effect on COX-2 expression and consequently PGE_2 production. We next addressed the question whether COX activity was inhibited. We performed COX-1 activity using Human Embryonic kidney (HEK)-293 cells stably overexpressing COX-1. Cells were treated with all compounds at 10 and 50 μM and PGE_2 was measured after the addition of arachidonic acid (AA). The results showed that compound **A5** had the maximal inhibitory effect on COX-1 activity with more than 80% inhibition at 50 μM (Fig. 2a) with an IC_{50} of 5.2 μM .

(See figure on next page.)

Fig. 1 Effects of the *gem*-difluorobisarylic derivatives on PGE_2 production and COX-2 expression in activated macrophages. BMDM were treated with 6 increasing concentrations, prior to the addition of 10 ng/mL LPS for 24 h. PGE_2 secretion was measured and expressed as percentage of LPS for **a** compounds **A1** and **A2** and **b** compounds **A3**, **A4** and **A5**. Corresponding IC_{50} fitting curves are shown. **c**, **d** COX-2 and β -actin expression in basal and LPS-treated BMDM with 50 μM of all compounds. Results are obtained from the same blot. Protein bands for basal or LPS-treated macrophages, in the absence of inhibitors, as shown in **c** and **d**, are identical for illustration purpose. Dose-response effect of compounds **e A4** and **f A5** on COX-2 expression. β -actin was used as loading control. Ratio of COX-2/ β -actin was calculated after densitometry analysis using ImageJ software. Data are represented as mean \pm SEM (n = 4), *p < 0.05 versus LPS (One-way Anova followed by the Dunnnett's test)



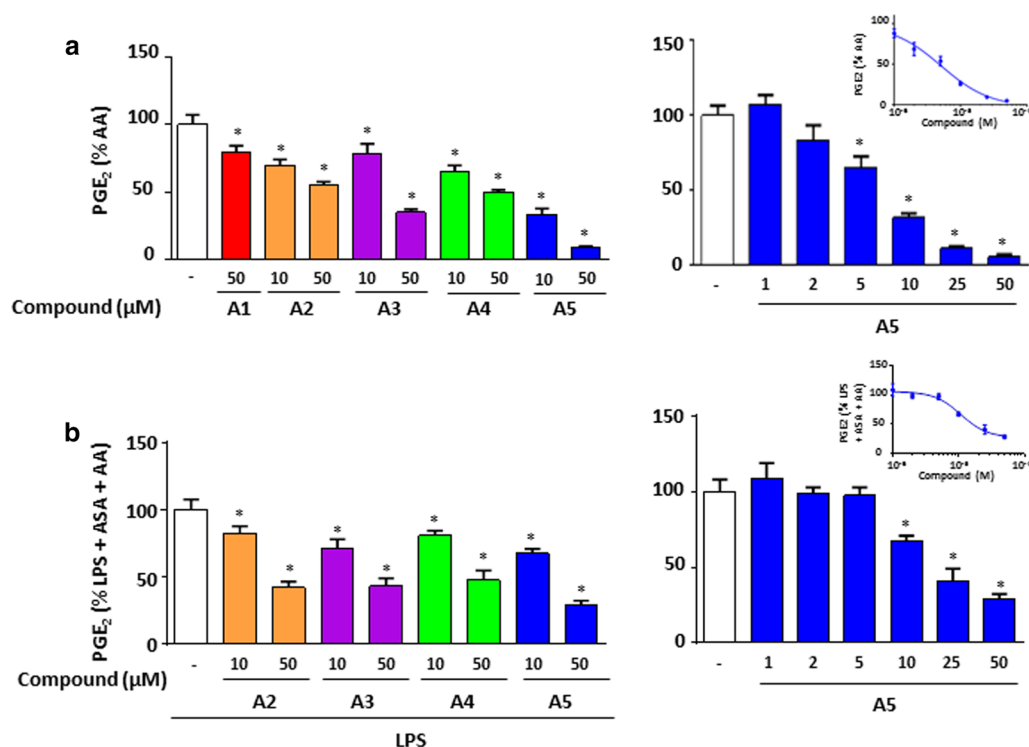


Fig. 2 Effects of the *gem*-difluorobisarylic derivatives on COX-1 and COX-2 activity. **a** COX-1 activity. HEK-293 cells overexpressing recombinant COX-1 were treated with 10 and 50 μM of all compounds for 45 min prior to the addition of 10 μM arachidonic acid (AA). PGE₂ was measured. **b** COX-2 activity. BMDM cells were treated with 10 μM of ASA for 30 min, washed, and 10 ng/mL LPS was added for 24 h to induce COX-2. Cells were further incubated with 10 and 50 μM of each compound prior to the addition of 10 μM AA. PGE₂ was measured. Data are represented as mean ± SEM (n = 4), *p < 0.05 versus AA for COX-1 activity, and versus LPS + ASA + AA for COX-2 activity (One-way Anova followed by the Dunnett's test)

COX-2 activity was also assessed on BMDM treated for 30 min with aspirin to inhibit basal COX activity prior to the addition of 10 ng/mL LPS for 24 h which induces COX-2. These cells were then treated with 10 and 50 μM of derivatives and further incubated with AA. PGE₂ production revealed that compound A5 inhibited strongly COX-2 activity with an IC₅₀ of 13.3 μM, whereas moderate effect was observed for compounds A2, A3 and A4 (Fig. 2b). Indeed, the assay used for COX-2 activity cannot exclude an effect on mPGES-1.

In parallel, we assessed the effect of these compounds on the production of IL-6 and NO measured by its breakdown product nitrite. Figure 3 showed a dose response inhibition of compounds A2 (Fig. 3a, c), A4

and A5 (Fig. 3b, d) for both IL-6 and NO secretion. IC₅₀ are presented in Table 2 and were significant for compounds A4 and A5.

NOS-II is the inducible form of nitric oxide synthase, and is responsible for the production of the measured NO. For this, NOS-II protein expression was analyzed in LPS-stimulated BMDM, treated with 50 μM of bisarylic derivatives for 24 h. Results revealed that the fluorinated compounds A2, A4 and A5 inhibited NOS-II expression in parallel to NO production (Fig. 3e, f).

Molecular docking

We finally carried out model analysis of the inhibitors with ovine COX-1 [13] and murine COX-2 [14], to examine how these compounds dock with the active sites of

(See figure on next page.)

Fig. 3 Effects of the *gem*-difluorobisarylic derivatives IL-6 and nitrite, and NOS-II expression. BMDM were treated with 6 increasing concentrations of all compounds prior to the addition of 10 ng/mL LPS for 24 h. IL-6 and NO production was measured and expressed as percentage of LPS for **a**, **c** compounds A1 and A2, and **b**, **d**, compounds A3, A4 and A5, respectively. Corresponding IC₅₀ fitting curves are shown. **e**, **f** NOS-II and β-actin expression in basal and LPS-treated BMDMs with 50 μM of all compounds. Results are obtained from the same blot. Protein bands for basal or LPS-treated in macrophages in the absence of inhibitors, as shown in **e** and **f**, are identical for illustration purpose. β-actin was used as loading control. Data are represented as mean ± SEM (n = 4), *p < 0.05 versus LPS (One-way Anova followed by the Dunnett's test)

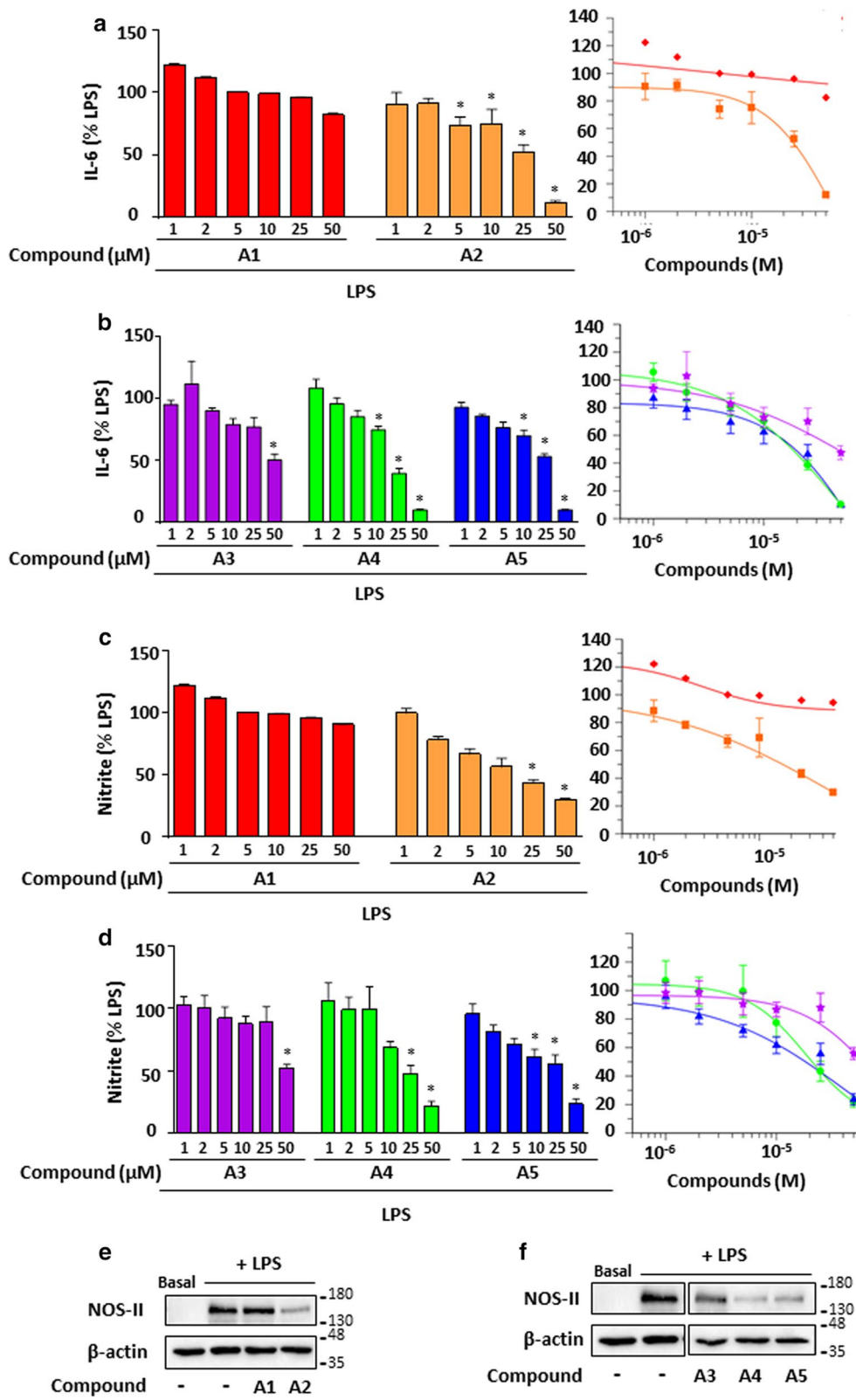


Table 2 In vitro inhibition activity of compounds **A1**, **A2**, **A3**, **A4** and **A5** on inflammatory mediators in macrophages

Compounds	IC ₅₀ (μM)	
	IL-6	NO
A1	ND	ND
A2	64.5 ± 21.1 ^a	45.2 ± 24.6
A3	60 ± 60.2	ND
A4	51.2 ± 17.4	18.5 ± 2.7
A5	82.6 ± 24.0	40.9 ± 25.4
Fenoprofen	300 ± 100	43.8 ± 39.2

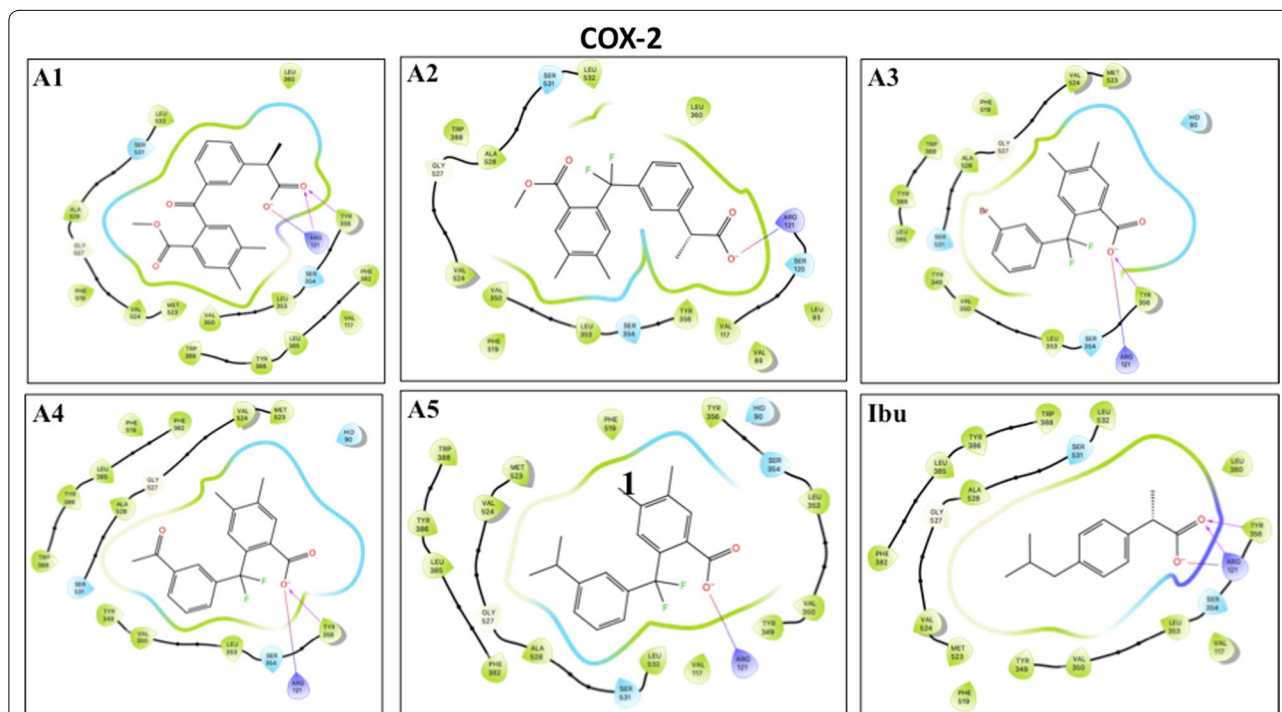
ND not determined

^a Mean ± SEM

the enzymes and to determine the amino acids involved in the interaction with the compounds. Ibuprofen docked into the hydrophobic cavity of COX-2 formed by Arg121, Tyr356, Ser354, Leu353, Val350 and Tyr349, where the carboxyl group of ibuprofen interacts with Arg121 and Tyr356 by a salt bridge and a hydrogen bond. The compounds **A3**, **A4** and **A5** were docked near Arg121, similarly to ibuprofen. Compounds **A3** and **A4** showed interaction with Tyr356 (Fig. 4). The binding scores of

compounds **A3**, **A4** and **A5** (−7.7 kcal/mol, −7.7 kcal/mol and −7.5 kcal/mol respectively) are comparable to ibuprofen (Table 3). Furthermore, the difluoromethyl group present in these compounds, which introduces a strong electrostatic field in this hydrophobic pocket, would be in favor the interaction with Arg121. Compounds **A1** and **A2**, even though they occupy the same active pocket, interact with Arg121 through the carboxylate group with less binding energy, have a bulky side chains that negatively would affect the stability of these molecules in the hydrophobic pocket. For COX-1, ibuprofen docked into the hydrophobic pocket composed of the amino acids Arg120, Tyr355, Ser353, Leu352, Val349, Tyr348, Val116, Leu531, Ser530, Ala527, Gly526 and Ile523. All compounds docked in the same active hydrophobic pocket of COX-1. Only Arg120 interacts with the carboxylate group by a salt bridge (Fig. 5). Similarly, to ibuprofen, compounds **A2**, **A3**, **A4** and **A5** showed a moderate binding energy compared to ibuprofen (−7 kcal/mol and −7.8 kcal/mol respectively, Table 3) whereas compound **A1** showed the lowest binding energy, which is compatible with biological activities.

More analyses are required to fully understand the key role of the fluorine atoms on the biological activity of these molecules. However, to explain these results, it is

**Fig. 4** Two-dimensional pose of compounds **A1** to **A5** and Ibuprofen inside the binding pocket of mouse COX-2 as crystallized by [13].

Ligand-receptor interactions as highlighted by Maestro (Shrodinger, LLC). Ligands are represented in stick, and amino acids within the binding pocket are labeled. An arrow represents the H-bonds between an amino acid and ligand groups. A line shows a potential salt bridge between two charged groups

Table 3 Comparison of COX-1 and COX-2 molecular docking data

Compound	COX-1 kcal/mol	COX-2 kcal/mol
A1	-6.5	-6.6
A2	-7	-6.7
A3	-7	-7.7
A4	-7	-7.7
A5	-7	-7.5
Ibuprofen	-7.8	-7.7

possible that the bulky and lipophilic CF_2 group could fit better in the pocket of these proteins than the carbonyl of ketoprofen or the oxygen atom of fenoprofen. Further, in the case of compounds **A3**, **A4** and **A5** it can also increase the acidity of the CO_2H in ortho position.

Conclusion

In conclusion, five bisarylic derivatives were prepared and tested in comparison with fenoprofen. This type of compounds is endowed with certain anti-inflammatory activities in mouse primary macrophages with a significant difference between the fluorinated analogues and the non-fluorinated one, showing the importance of the CF_2 group. All fluorinated derivatives blocked PGE_2 , nitrite and IL-6 production in activated macrophages.

Derivatives **A4** and **A5** showed additional strong inhibition of COX-2 and NOS-II expression. In addition, derivatives **A3**, **A4** and **A5** showed better anti-inflammatory activities than the other derivatives, with compound **A5** having COX-1 and COX-2 direct inhibitory activities. Molecular docking of the compounds COX-1 and COX-2 are in support of the biological activity.

Methods

Chemistry experimental part

Reactions were carried out as described previously and monitored as described by ^{19}F NMR and by thin-layer chromatography (TLC) [15]. Yields refer to chromatographically and spectroscopically (^1H , ^{13}C , and ^{19}F NMR) homogeneous materials. Nuclear magnetic resonance (NMR) spectra have been recorded as previously described [15]. Mass spectral analyses have been performed at the Centre Régional de Mesures Physiques de l'Ouest (CRMPO) in Rennes (France).

Synthesis of methyl 4-(3-bromophenyl)-4-hydroxybut-2-ynoate **4**

To a solution of methylpropiolate (2.6 mL, 29.20 mmol, 1.2 equiv.) in anhydrous THF (20 mL) cooled at -90°C and set under nitrogen, *n*-BuLi (11.4 mL, 2.5 M, 1.2 equiv.) was added dropwise. The reaction mixture was stirred for 30 min at $T = -80^\circ\text{C}$ before the dropwise addition of a solution of 3-bromobenzaldehyde (4 g, 21.60 mmol)

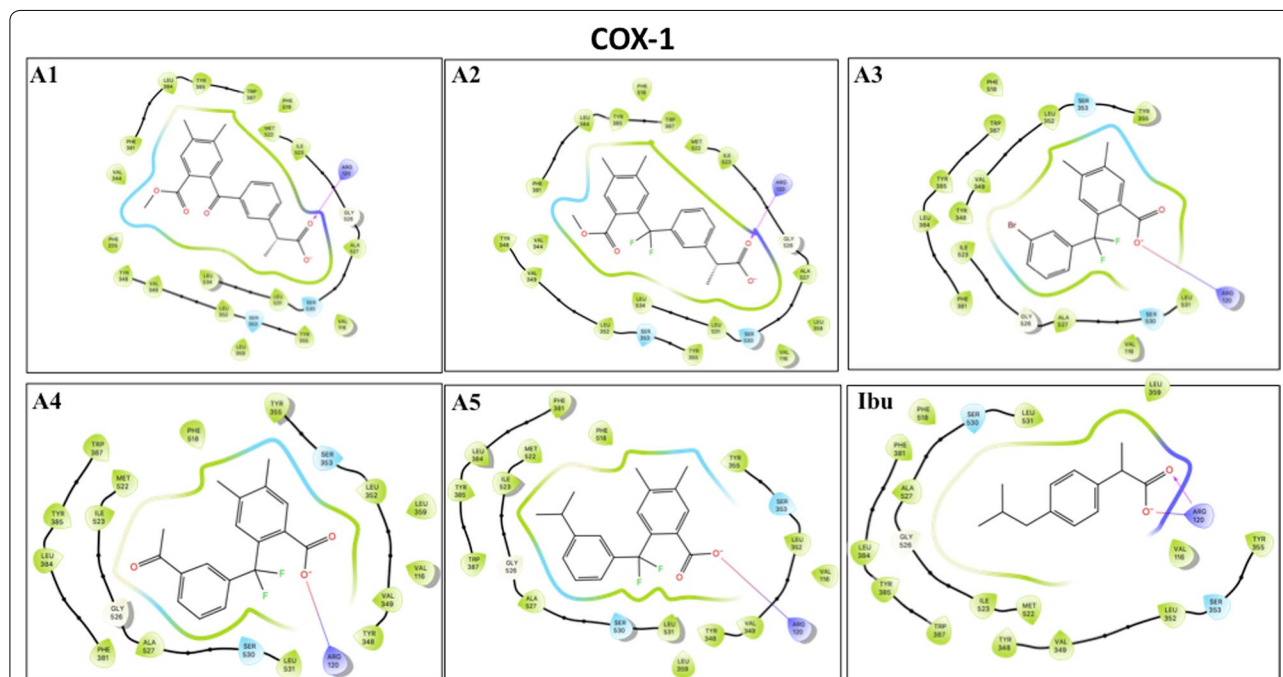


Fig. 5 Two-Dimensional pose of compounds **A1** to **A5** and Ibuprofen inside the binding pocket of human COX-1 as crystallized by [14]. Ligand receptor interactions were evaluated for COX-1 as described in legend for Fig. 4

in anhydrous THF (20 mL). After stirring for additional 20 min at the same temperature, TMSCl (7 mL, 55.00 mmol, 2.5 equiv.) was added dropwise to the reaction mixture that was stirred for 1 h at $-80\text{ }^{\circ}\text{C}$ and then left to rise at room temperature while continuous stirring for additional 2 h. The mixture was treated with concentrated solution of NH_4Cl , extracted with ethyl acetate (3 times), dried over Na_2SO_4 and concentrated by evaporating the solvent. Alcohol **4** was isolated over silica gel by column chromatography.

Synthesis of methyl 4-(3-bromophenyl)-4-oxobut-2-ynoate **5**

To alcohol **4** (2.1 g, 7.46 mmol) in acetone (18 mL) was added dropwise under magnetic stirring at room temperature, a concentrated (5.4 M) solution of Jones reagent until disappearance of the starting material (TLC analysis). After addition of isopropanol (5 equiv.), the reaction mixture was filtered, and the filtrate was extracted with ethyl acetate. The combined organic phases were dried over Na_2SO_4 , filtered and concentrated in vacuum. After purification by chromatography on silica gel, ketone **5** was obtained.

Synthesis of methyl 4-(3-bromophenyl)-4,4-difluorobut-2-ynoate **8**

To propargylic ketone **5** (350 mg, 1.31 mmol) were added one drop of 95% ethanol and DAST (1.05 mL, 7.96 mmol, 6 equiv.). The reaction mixture was stirred at $60\text{ }^{\circ}\text{C}$ for 7 h. After coming back to room temperature and hydrolysis, the reaction mixture was extracted with ethyl acetate (3 times). The organic layers were separated, washed with water (3 times), dried over Na_2SO_4 and concentrated under vacuum. After purification by chromatography on silica gel, fluorinated compound **8** was obtained.

Synthesis of methyl 2-(3-bromobenzoyl)-4,5-dimethylcyclohexa-1,4-dienecarboxylate **6** and methyl 2-((3-bromophenyl) difluoromethyl)-4,5-dimethylcyclohexa-1,4-dienecarboxylate **9**

Difluoro propargylic ester (1.54 mmol) and 2,3-dimethyl-1,3-butadiene (14 equiv.) were refluxed neat at nearly $80\text{ }^{\circ}\text{C}$. The reaction was controlled by ^{19}F NMR after 5 h and was stopped by that time. Finally, the unreacted butadiene was evaporated. After purification by column chromatography on silica gel, cyclohexadienes **6** and **9** were isolated.

Synthesis of methyl 2-(3-bromobenzoyl)-4,5-dimethylbenzoate **7** and methyl 2-((3-bromophenyl) difluoromethyl)-4,5-dimethylbenzoate **10**

A solution of the cyclohexadiene (2.18 mmol) and DDQ (1.2 equiv.) in toluene (7 mL) was stirred at $42\text{ }^{\circ}\text{C}$ for 2 h.

The reaction mixture was filtered on silica gel and the residues were washed with ethyl acetate. The organic phase was concentrated in vacuo and compounds **7** and **10** were isolated by chromatography on silica gel.

Synthesis of methyl 4,5-dimethyl-2-(3-(prop-1-en-2-yl) benzoyl) benzoate **11** and methyl 2-(difluoro(3-(prop-1-en-2-yl) phenyl) methyl)-4,5-dimethylbenzoate **12**

A solution of bromo-ester (1.74 mmol), isopropenylboronic acid pinacol ester (2 equiv.), palladium dichlorobis-triphenylphosphine (5% mol) and potassium carbonate (2 equiv.) in a 5/1 mixture of dioxane and water (15/3 mL) was stirred at $90\text{ }^{\circ}\text{C}$ for 20 h. The reaction mixture was extracted by ethyl acetate (3 times). The combined organic phases were washed with water, dried over Na_2SO_4 and concentrated in vacuo. After purification by chromatography on silica gel, the compounds **11** and **12** were isolated.

Synthesis of methyl 2-(3-(1-hydroxypropan-2-yl) benzoyl)-4,5-dimethylbenzoate **13** and methyl 2-(difluoro(3-(1-hydroxypropan-2-yl)phenyl) methyl)-4,5-dimethylbenzoate **14**

To the alkene (0.72 mmol) in anhydrous THF (5 mL) was added, dropwise under magnetic stirring and under N_2 at $0\text{ }^{\circ}\text{C}$, a solution of BH_3 in THF (5.5 equiv.). The reaction mixture was stirred overnight at room temperature. After 24 h, the mixture was oxidized by addition of H_2O_2 30% (4.4 equiv.) and NaOH 3 M (4.4 equiv.) and was stirred for 2 h. The organic phase was separated, while the aqueous phase was extracted by ethyl acetate. The organic fractions were collected, dried over Na_2SO_4 , and concentrated in vacuo. After purification by flash chromatography on silica gel, alcohols **13** and **14** were isolated.

Synthesis of (2-((3-bromophenyl)difluoromethyl)-4,5-dimethylphenyl)methanol **15**, (2-(difluoro(3-(prop-1-en-2-yl) phenyl)methyl)-4,5-dimethylphenyl)methanol **16** and (2-(difluoro(3-isopropylphenyl)methyl)-4,5-dimethylphenyl)methanol **18**

To the ester (0.27 mmol) in anhydrous THF (4 mL) was added, dropwise under magnetic stirring and under N_2 at $0\text{ }^{\circ}\text{C}$, a 1 M solution of LiEt_3BH in THF (2.5 equiv.). The reaction mixture was stirred at $0\text{ }^{\circ}\text{C}$ for 15 min and then quenched by addition of a saturated NH_4Cl solution. The organic phase was separated, while the aqueous phase was extracted by ethyl acetate. The organic fractions were collected, dried over Na_2SO_4 , and concentrated in vacuo. After purification by flash chromatography on silica gel, alcohols **15**, **16** and **18** were isolated.

Synthesis of methyl 2-(difluoro(3-isopropylphenyl)methyl)-4,5-dimethylbenzoate 17

To a solution of **12** (498 mg, 1.51 mmol) in AcOEt (15 mL), was added 50 mg of palladium-charcoal catalyst (10%). The mixture was stirred at room temperature under hydrogen atmosphere. After 2 h, it was filtered and compound **17** was obtained, after purification on silica gel.

The physicochemical properties and the spectral data of intermediates **4–18** are presented in the Tables 4 and 5, respectively and in Tables 6 and 7 for the synthesized bisarylic derivatives **A1** to **A5**.

Synthesis of gem-difluorobisarylic derivatives **A1**, **A2**, **A3**, **A4** and **A5**

To alcohol in acetone was added dropwise under magnetic stirring at room temperature, a concentrated (5.4 M) solution of Jones reagent until disappearance of the starting material (TLC analysis). After addition of

isopropanol (5 equiv.), the reaction mixture was filtered, and the filtrate was extracted with ethyl acetate. The combined organic phases were dried over Na₂SO₄, filtered and concentrated in vacuum. After purification by chromatography on silica gel, carboxylic acid was obtained.

Supporting information

Experimental details and characterization data of new compounds with copies of ¹H, ¹³C and ¹⁹F NMR spectra are presented in the supplementary section, Additional file 1.

Evaluation of inflammation in macrophages

C57BL/6J male mice (20–25 g, 8 week-old) were obtained from Charles River (Ecully, France) and the animal facility of the American University of Beirut. Mice were housed 5 per cage in temperature- and humidity-controlled rooms, kept on a 12-h light–dark cycle, and provided with standard food and water ad lib and with enrichment

Table 4 The physicochemical properties of intermediates **4–18**

Compound	IUPAC Name	Aspect	Mass of the starting material	Mass of the product	Rf value (PE:EtOAc)	m.p. (°C)	% yield
4	Methyl 4-(3-bromophenyl)-4-hydroxybut-2-ynoate	Yellow oil	4 g	3.9 g	0.30 (8:2)	–	70
5	Methyl 4-(3-bromophenyl)-4-oxobut-2-ynoate	Yellow solid	2.10 g	1.59 g	0.40 (9:1)	102–104	80
6	Methyl 2-(3-bromobenzoyl)-4,5-dimethylcyclohexa-1,4-dienecarboxylate	Yellow solid	410 mg	560 mg	0.43 (9:1)	100–102	96
7	Methyl 2-(3-bromobenzoyl)-4,5-dimethylbenzoate	Yellow solid	937 mg	810 mg	0.34 (9:1)	122–124	87
8	Methyl 4-(3-bromophenyl)-4,4-difluorobut-2-ynoate	Colorless oil	350 mg	270 mg	0.44 (9:1)	–	71
9	Methyl 2-((3-bromophenyl)difluoromethyl)-4,5-dimethylcyclohexa-1,4-dienecarboxylate	White solid	757 mg	925 mg	0.44 (9:1)	72–74	95
10	Methyl 2-((3-bromophenyl)difluoromethyl)-4,5-dimethylbenzoate	Yellow solid	808 mg	731 mg	0.51 (9:1)	60–62	91
11	Methyl 4,5-dimethyl-2-(3-(prop-1-en-2-yl)benzoyl)benzoate	White solid	782 mg	640 mg	0.34 (9:1)	82–48	92
12	Methyl 2-(difluoro(3-(prop-1-en-2-yl)phenyl)methyl)-4,5-dimethylbenzoate	Yellow oil	640 mg	539 mg	0.35 (9:1)	–	94
13	Methyl 2-(3-(1-hydroxypropan-2-yl)benzoyl)-4,5-dimethylbenzoate	Yellow oil	400 mg	309 mg	0.42 (7:3)	–	73
14	Methyl 2-(difluoro(3-(1-hydroxypropan-2-yl)phenyl)methyl)-4,5-dimethylbenzoate	Yellow oil	240 mg	192 mg	0.36 (7.5:2.5)	–	76
15	2-((3-bromophenyl)difluoromethyl)-4,5-dimethylphenylmethanol	White solid	100 mg	88 mg	0.26 (9:1)	62–64	95
16	2-(difluoro(3-(prop-1-en-2-yl)phenyl)methyl)-4,5-dimethylphenylmethanol	Yellow oil	148 mg	88 mg	0.37 (8:2)	–	65
17	Methyl 2-(difluoro(3-isopropylphenyl)methyl)-4,5-dimethylbenzoate	White solid	498 mg	476 mg	0.72 (9:1)	116–118	95
18	2-(difluoro(3-isopropylphenyl)methyl)-4,5-dimethylphenylmethanol	White solid	294 mg	260 mg	0.69 (9:1)	80–82	96

Table 5 Spectral data of intermediates 4–18

Compound	¹ H NMR	¹³ C NMR	¹⁹ F NMR
4	CDCl₃, 300 MHz: 7.56 (m, 1H), 7.36 (m, 2H), 7.18 (m, 1H), 5.44 (s, 1H), 3.70 (s, 3H), 3.64 (br. s, 1H)	CDCl₃, 75 MHz: 153.7, 140.5, 131.8, 130.2, 129.6, 125.1, 122.7, 86.0, 77.6, 63.2, 53.0	
5	CDCl₃, 300 MHz: 8.02 (t, 1H, J = 1.7 Hz), 7.86 (ddd, 1H, J = 7.9, 1.7 and 1.0 Hz), 7.61 (ddd, 1H, J = 7.9, 1.7 and 1.0 Hz), 7.23 (t, 1H, J = 7.9 Hz), 3.73 (s, 3H)	CDCl₃, 75 MHz: 173.6, 151.4, 137.0, 136.1, 131.3, 129.5, 127.4 (3C), 79.7, 78.3, 52.6	
6	CDCl₃, 300 MHz: 8.01 (t, 1H, J = 1.9 Hz), 7.80 (m, 1H), 7.68 (m, 1H), 7.33 (t, 1H, J = 7.8 Hz), 3.53 (s, 3H), 2.97–2.98 (m, 4H), 1.74 (s, 3H), 1.67 (s, 3H)	CDCl₃, 75 MHz: 197.1, 165.9, 146.8, 137.0, 136.0, 131.2, 130.3, 127.1, 125.6, 123.1, 123.0, 120.6, 51.8, 36.5, 32.6, 18.2, 17.8	
7	CDCl₃, 300 MHz: 7.89 (t, 1H, J = 1.7 Hz), 7.81 (s, 1H), 7.62 (m, 2H), 7.27 (t, 1H, J = 7.9 Hz), 7.13 (s, 1H), 3.61 (s, 3H), 2.36 (s, 3H), 2.33 (s, 3H)	CDCl₃, 75 MHz: 195.9, 166.3, 142.1, 139.3, 138.8, 138.6, 135.6, 131.8, 131.1, 129.9, 128.8, 127.7, 126.4, 122.7, 52.0, 19.9, 19.6	
8	CDCl₃, 300 MHz: 7.70 (s, 1H), 7.55 (m, 1H), 7.49 (m, 1H), 7.26 (t, 1H, J = 8.0 Hz), 3.76 (s, 3H)	CDCl₃, 75 MHz: 152.1 (t, ⁴ J = 2.4 Hz), 136.2 (t, ² J = 27.5 Hz), 134.5 (t, ⁴ J = 1.6 Hz), 130.4, 128.3 (t, ³ J = 5.0 Hz), 123.9 (t, ³ J = 4.9 Hz), 122.7, 110.4 (t, ³ J = 236.3 Hz), 78.4 (t, ³ J = 5.9 Hz), 76.5 (t, ² J = 43.7 Hz), 53.4	CDCl₃, 282 MHz: -80.06 (s)
9	CDCl₃, 300 MHz: 7.70 (s, 1H), 7.50 (s, 1H), 7.48 (s, 1H), 7.23 (m, 1H), 3.68 (s, 3H), 2.86 (t, 2H, J = 7.2 Hz), 2.50 (t, 2H, J = 7.2 Hz), 1.57 (s, 3H), 1.52 (s, 3H)	CDCl₃, 75 MHz: 170.3, 137.7 (t, ² J = 28.4 Hz), 133.2, 130.0, 129.9 (t, ³ J = 5.0 Hz), 128.9 (t, ³ J = 5.9 Hz), 128.8 (t, ² J = 25.4 Hz), 124.5 (t, ⁴ J = 5.6 Hz), 122.5, 121.6, 121.2, 119.4 (t, ³ J = 244.4 Hz), 52.1, 35.8, 31.6, 18.0, 17.7	CDCl₃, 282 MHz: -93.06 (s)
10	CDCl₃, 300 MHz: 7.62 (s, 1H), 7.54 (m, 1H), 7.49 (s, 1H), 7.47 (s, 1H), 7.40 (m, 1H), 7.26 (m, 1H), 3.65 (s, 3H), 2.36 (s, 3H), 2.33 (s, 3H)	CDCl₃, 75 MHz: 168.2, 140.1 (t, ² J = 28.3 Hz), 140.0, 139.1 (t, ⁴ J = 1.3 Hz), 132.8 (t, ⁴ J = 2.7 Hz), 131.9 (t, ² J = 26.9 Hz), 131.1, 129.7, 129.0 (t, ³ J = 5.3 Hz), 128.5 (t, ³ J = 7.9 Hz), 128.4 (t, ³ J = 3.4 Hz), 124.6 (t, ³ J = 5.0 Hz), 122.1, 119.7 (t, ³ J = 242.3 Hz), 52.1, 19.9, 19.4	CDCl₃, 282 MHz: -82.83 (s)
11	CDCl₃, 300 MHz: 7.93 (t, 1H, J = 1.6 Hz), 7.80 (s, 1H), 7.64 (ddd, 1H, J = 7.7, 1.6, 1.2 Hz), 7.53 (dt, 1H, J = 7.7, 1.2 Hz), 7.35 (t, 1H, J = 7.7 Hz), 7.18 (s, 1H), 5.38 (m, 1H), 5.12 (m, 1H), 3.56 (s, 3H), 2.37 (s, 3H), 2.34 (s, 3H), 2.15 (m, 3H)	CDCl₃, 75 MHz: 197.3, 166.7, 142.4, 141.9, 141.6, 139.2, 138.6, 137.5, 131.0, 129.9, 129.1, 128.6, 128.3, 126.8, 125.8, 113.5, 51.9, 21.7, 19.9, 19.6	
12	CDCl₃, 300 MHz: 7.55 (s, 1H), 7.42 (m, 1H), 7.38 (s, 1H), 7.36 (s, 1H), 7.26 (m, 1H), 7.24 (m, 1H), 5.29 (m, 1H), 5.03 (m, 1H), 3.54 (s, 3H), 2.25 (s, 3H), 2.23 (s, 3H), 2.06 (m, 3H)	CDCl₃, 75 MHz: 168.6, 142.7, 141.2, 139.7, 138.8, 137.8 (t, ² J = 27.6 Hz), 132.5 (t, ² J = 27.3 Hz), 130.7, 128.7 (t, ³ J = 3.4 Hz), 128.6 (t, ³ J = 7.6 Hz), 128.0, 126.8 (t, ⁴ J = 1.9 Hz), 125.0 (t, ³ J = 5.2 Hz), 122.9 (t, ³ J = 5.2 Hz), 120.6 (t, ³ J = 241.6 Hz), 113.2, 52.0, 21.7, 19.9, 19.3	CDCl₃, 282 MHz: -82.49 (s)
13	CDCl₃, 300 MHz: 7.77 (s, 1H), 7.67 (t, 1H, J = 1.6 Hz), 7.54 (dt, 1H, J = 7.5, 1.6 Hz), 7.42 (dt, 1H, J = 7.5, 1.6 Hz), 7.36 (t, 1H, J = 7.5 Hz), 7.20 (s, 1H), 3.70 (d, 2H, J = 6.9 Hz), 3.51 (s, 3H), 2.97 (sext, 1H, J = 6.9 Hz), 2.37 (s, 3H), 2.34 (s, 3H), 1.71 (br. s, 1H), 1.26 (d, 3H, J = 6.9 Hz)	CDCl₃, 75 MHz: 197.3, 167.0, 144.4, 141.9, 139.0, 138.7, 137.8, 132.2, 130.9, 129.2, 128.7, 127.8 (2C), 127.1, 68.4, 51.9, 42.3, 19.9, 19.6, 17.5197.3, 167.0, 144.4, 141.9, 139.0, 138.7, 137.8, 132.2, 130.9, 129.2, 128.7, 127.8 (2C), 127.1, 68.4, 51.9, 42.3, 19.9, 19.6, 17.5	
14	CDCl₃, 300 MHz: 7.43 (s, 1H), 7.32 (s, 1H), 7.25 (s, 1H), 7.23 (s, 2H), 7.16–7.21 (m, 1H), 3.53 (d, 2H, J = 6.9 Hz), 3.46 (s, 3H), 2.83 (sext, 1H, J = 6.9 Hz), 2.24 (s, 3H), 2.21 (s, 3H), 2.14 (br. s, 1H), 1.14 (d, 3H, J = 6.9 Hz)	CDCl₃, 75 MHz: 168.7, 143.9, 139.7, 138.8, 137.7 (t, ² J = 27.4 Hz), 132.4 (t, ² J = 27.3 Hz), 130.6, 128.8 (t, ⁴ J = 1.7 Hz), 128.7 (t, ³ J = 3.5 Hz), 128.3 (t, ² J = 7.7 Hz), 128.2, 125.1 (t, ³ J = 5.1 Hz), 124.1 (t, ³ J = 5.2 Hz), 120.4 (t, ³ J = 241.3 Hz), 68.3, 52.0, 42.2, 19.8, 19.3, 17.3	CDCl₃, 282 MHz: -82.21 (s)
15	CDCl₃, 300 MHz: 7.52 (m, 1H), 7.74 (m, 1H), 7.28 (m, 1H), 7.26 (m, 1H), 7.14–7.19 (m, 2H), 4.43 (s, 2H), 2.21 (s, 3H), 2.19 (s, 3H), 1.82 (s, 1H)	CDCl₃, 75 MHz: 139.5 (t, ⁴ J = 1.5 Hz), 139.5 (t, ² J = 28.8 Hz), 136.2 (t, ³ J = 2.1 Hz), 135.8, 133.3 (t, ⁴ J = 1.8 Hz), 130.9, 130.4 (t, ² J = 26.2 Hz), 130.0, 129.1 (t, ³ J = 5.2 Hz), 127.8 (t, ³ J = 7.9 Hz), 124.7 (t, ³ J = 5.2 Hz), 122.5, 120.8 (t, ³ J = 241.8 Hz), 62.0 (t, ³ J = 3.4 Hz), 19.5 (2C)	CDCl₃, 282 MHz: -83.28 (s)

Table 5 (continued)

Compound	¹ H NMR	¹³ C NMR	¹⁹ F NMR
16	CDCl₃, 300 MHz: 7.53 (s, 1H), 7.45 (m, 1H), 7.29 (s, 1H), 7.25 (m, 1H), 7.21 (s, 2H), 5.29 (s, 1H), 5.05 (t, 1H, J = 1.4 Hz), 4.48 (s, 2H), 2.23 (s, 3H), 2.20 (s, 3H), 2.06 (dd, 3H, J = 1.4, 0.8 Hz)	CDCl₃, 75 MHz: 142.5, 141.6, 139.3, 137.4 (t, ² J = 28.0 Hz), 136.3 (t, ⁴ J = 2.1 Hz), 135.7, 131.3 (t, ² J = 26.5 Hz), 131.1, 128.3, 128.0 (t, ³ J = 7.8 Hz), 127.3 (t, ³ J = 1.8 Hz), 125.1 (t, ³ J = 5.2 Hz), 122.9 (t, ³ J = 5.2 Hz), 121.7 (t, ¹ J = 241.5 Hz), 113.5, 62.2 (t, ⁴ J = 3.2 Hz), 21.7, 19.5 (2C)	CDCl₃, 282 MHz: - 82.87 (s)
17	(CDCl₃, 500 MHz): 7.44 (s, 1H), 7.42 (s, 1H), 7.36 (s, 1H), 7.23–7.29 (m, 2H), 7.21 (m, 1H), 3.57 (s, 3H), 2.9 (sext, 1H, J = 6.9 Hz), 2.31 (s, 3H), 2.30 (s, 3H), 1.23 (d, 6H, J = 6.9 Hz)	(CDCl₃, 125 MHz): 168.7, 148.8, 139.6, 138.7, 137.7 (t, ² J = 27.3 Hz), 132.6 (t, ² J = 27.3 Hz), 130.7, 128.8 (t, ³ J = 3.4 Hz), 128.6 (t, ³ J = 7.6 Hz), 128.0, 127.8 (t, ⁴ J = 1.8 Hz), 123.9 (t, ³ J = 5.0 Hz), 123.6 (t, ³ J = 5.2 Hz), 120.7 (t, ¹ J = 241.2 Hz), 52.0, 34.1, 23.9 (2C), 19.9, 19.4	(CDCl₃, 470 MHz): - 81.94 (s)
18	CDCl₃, 300 MHz: 7.25 (s, 1H), 7.23 (s, 1H), 7.16 (s, 1H), 7.14 (s, 1H), 7.12 (m, 1H), 7.05 (m, 1H), 4.39 (s, 2H), 2.76 (sext, 1H, J = 6.9 Hz), 2.41 (br. s, 1H), 2.13 (s, 3H), 2.12 (s, 3H), 1.1 (d, 6H, J = 6.9 Hz)	CDCl₃, 75 MHz: 149.11389, 137.3 (t, ² J = 27.8 Hz), 136.4, 135.2, 131.1 (t, ² J = 26.5 Hz), 130.5, 128.3, 128.0 (t, ⁴ J = 1.7 Hz), 127.7 (t, ³ J = 7.8 Hz), 123.9 (t, ³ J = 5.0 Hz), 123.6 (t, ³ J = 5.2 Hz), 121.7 (t, ¹ J = 240.8 Hz), 61.6 (t, ⁴ J = 3.2 Hz), 33.9, 23.7 (2C), 19.3 (2C)	CDCl₃, 282 MHz: - 82.66 (s)

Table 6 The physicochemical properties of synthesized bisaryl derivatives A1 to A5

Compound	IUPAC Name	Aspect	Mass of the starting material (mg)	Mass of the product	Rf value (PE:EtOAc)	m.p. (°C)	% yield
A1	2-(3-(2-benzoyl-4,5-dimethylbenzoyl)phenyl)propanoic acid	White solid	270	225	0.17 (5:5)	86–88	80
A2	2-(3-(difluoro(2-(methoxycarbonyl)-4,5-dimethylphenyl)methyl)phenyl)propanoic acid	White solid	74	60	0.40 (9.5:0.5)	98–100	78
A3	2-((3-bromophenyl)difluoromethyl)-4,5-dimethylbenzoic acid	White solid	100	83	0.28 (6:4)	64–66	80
A4	2-((3-acetylphenyl)difluoromethyl)-4,5-dimethylbenzoic acid	White solid	103	80	0.38 (8:2)	118–120	74
A5	2-(difluoro(3-isopropylphenyl)methyl)-4,5-dimethylbenzoic acid	White solid	100	55	0.26 (7:3)	152–154	53

environment (cotton cocoon) in the animal facility of the American University of Beirut. Body weight and food intake were monitored three times a week throughout the study period. ARRIVE guidelines were followed (Additional file 2). Approval for use of animals was obtained from the Institutional Animal Care and Use Committee of the American University of Beirut (IACUC # 16-09-m379).

On the day of the procedure, 2–3 mice were euthanized after 3 min exposure to carbon dioxide. BMDM were isolated as previously described and were plated at 0.8 million cells per well [16]. Flow cytometry analysis was performed using F4/80 -APC antibody (BioLegend 123115) and showed 90% macrophages. BMDM were then treated for 24 h with different concentrations of the bisaryl derivative compounds for 30 min prior to the addition of 10 ng/mL LPS. DMSO concentration did not exceed 0.4% with no effect. The supernatants were assessed for IL-6, PGE₂ and nitrite, the stable derivative of NO. Cells were washed with PBS and lysed in RIPA buffer containing inhibitors of protease. Total protein concentration was determined using DC protein assay (Bio-Rad 500-0115) with BSA as standard. IL-6, nitrite and PGE₂ were measured as described previously [17]. Western blot of NOS-II and COX-2 was performed as previously described [17–19]. 10 µg of total protein was assessed. The primary antibodies were developed and characterized as previously described: for COX-2, mouse monoclonal antibody anti-COX-2 (clone COX-214, 1/5000) [20]; for NOS-II, rabbit polyclonal antibody anti-NOS-II (dilution 1/2000) [21], and mouse β-actin (dilution 1/10,000) (Sigma-Aldrich A5441). Clarity™ western ECL substrate (Bio-Rad 170-5061) was used according to the manufacturer's instructions to reveal positive bands visualized using Bio-Rad ChemiDoc.

COX-1 and COX-2 activities

For COX-1 activity, human embryonic kidney (HEK)-293 cells (ATCC CRL-1573, Manassas, VA USA) stably

overexpressing human recombinant COX-1 were used [17]. Cells were treated with compounds A1 to A5 for 45 min in Hanks buffer and then 10 µM arachidonic acid (AA) were added for 30 min. PGE₂ was measured and corresponded to the breakdown metabolism of PGH₂ and PGE₂.

For COX-2 activity, BMDM were treated with 10 µM acetylsalicylic acid (ASA) for 30 min to irreversibly inhibit COX-1 and then washed and treated with LPS 10 ng/mL for 24 h. BMDM were treated with compounds A1 to A5 for 45 min in Hanks buffer, pH 7.4 containing 1 mg/mL BSA prior to the addition of 10 µM of AA for 30 min. Supernatants were collected and PGE₂ was determined.

Toxicity assay

WST-1 assay was used to determine the toxicity of the synthesized compounds (Cell proliferation WST-1 assay, Sigma-Aldrich 5015944001). Briefly, macrophages (50,000 cells per well) were plated in a 96 well plate in RPMI culture medium containing 10% FBS and grown for 24 h. Cells (in triplicates) were treated at 25 and 50 µM of the tested compounds. Culture medium without cells and cells without treatment were used as control. Results were expressed as percentage of cells without treatment. All compounds showed 95% viability at 50 µM.

Molecular docking

Target and small molecule preparation

All small molecules (A1 to A5) were built using Openbabel chemical toolbox (PMID: 21982300) and subsequent low energy 3D conformations were generated using Frog2 (PMID: 20444874). Protonation state corresponded to a pH of 7. The 3D structure of the ovine COX-1 (PDBID:

Table 7 Spectral data of synthesized bisarylic derivatives A1 to A5

Compound	¹ H NMR	¹³ C NMR (CDCl ₃ , 75 MHz)	¹⁹ F NMR (CDCl ₃ , 282 MHz)	HRMS (ESI)
A1	CDCl₃, 300 MHz: 7.78 (m, 2H), 7.53 (m, 2H), 7.36 (t, 1H, <i>J</i> = 7.7 Hz), 7.17 (s, 1H), 3.77 (quad, 1H, <i>J</i> = 7.2 Hz), 3.51 (s, 3H), 2.36 (s, 3H), 2.33 (s, 3H), 1.51 (d, 3H, <i>J</i> = 7.2 Hz)	CDCl₃, 75 MHz: 197.0, 179.7, 166.7, 141.9, 140.2, 138.9, 138.7, 137.9, 132.0, 131.0, 129.2, 128.7, 128.6, 128.1, 126.8, 51.9, 45.1, 19.9, 19.6, 18.0		calcd. For C ₂₀ H ₂₀ O ₅ Na: m/z [M + Na] ⁺ 363.12029; found: 363.1203 (0 ppm); C ₂₀ H ₁₉ O ₅ Na ₂ : m/z [M-H + 2Na] ⁺ 385.10224; found: 385.1014 (2 ppm).
A2	CDCl₃, 300 MHz: 7.44–7.46 (m, 3H), 7.33–7.40 (m, 3H), 3.76 (quad, 1H, <i>J</i> = 7.1 Hz), 3.56 (s, 3H), 2.33 (s, 3H), 2.32 (s, 3H), 1.50 (d, 3H, <i>J</i> = 7.2 Hz)	CDCl₃, 75 MHz: 179.6, 168.5, 139.8, 139.7, 138.9, 138.3 (t, ² <i>J</i> = 27.7 Hz), 132.3 (t, ² <i>J</i> = 27.1 Hz), 130.8, 128.9 (t, ⁴ <i>J</i> = 1.7 Hz), 128.7 (t, ³ <i>J</i> = 3.4 Hz), 128.5 (2C), 125.2 (t, ³ <i>J</i> = 5.1 Hz), 120.4 (t, ¹ <i>J</i> = 241.6 Hz), 68.3, 52.0, 45.2, 19.9, 19.4, 18.1	CDCl₃, 282 MHz: – 82.30 (s)	calcd. For C ₂₀ H ₂₀ F ₂ O ₄ Na: m/z [M + Na] ⁺ 385.12219; found: 385.1223 (0 ppm); C ₂₀ H ₁₉ O ₄ F ₂ Na ₂ : m/z [M + Na] ⁺ 407.10413; found: 407.1045 (0 ppm).
A3	deuterated acetone, 300 MHz: 7.29–7.63 (m, 6H), 2.22 (s, 3H), 2.20 (s, 3H)	deuterated acetone, 75 MHz: 170.0, 142.4 (t, ² <i>J</i> = 28.6 Hz), 141.7, 141.1 (t, ⁴ <i>J</i> = 1.3 Hz), 134.6 (t, ³ <i>J</i> = 1.7 Hz), 133.7 (t, ² <i>J</i> = 26.9 Hz), 132.7, 132.1, 131.3, 130.7 (t, ³ <i>J</i> = 5.3 Hz), 130.0 (t, ³ <i>J</i> = 8.0 Hz), 126.8 (t, ³ <i>J</i> = 5.3 Hz), 123.4, 122.0 (t, ¹ <i>J</i> = 241.6 Hz), 20.8, 20.4	CDCl₃, 282 MHz: – 82.34 (s)	calcd. For C ₁₆ H ₁₃ O ₂ F ₂ BrNa: m/z [M + Na] ⁺ 376.99592; found: 376.9958 (0 ppm); C ₁₆ H ₁₂ O ₂ F ₂ BrNa ₂ : m/z [M-H + 2Na] ⁺ 398.97786; found: 398.9779 (0 ppm); C ₁₆ H ₁₂ O ₂ F ₂ BrNa: m/z [M-HF + Na] ⁺ 356.98969; found: 356.9905 (2 ppm)
A4	deuterated acetone, 300 MHz: 8.18 (m, 1H), 8.07 (m, 1H), 7.77 (m, 1H), 7.56–7.61 (m, 3H), 2.60 (s, 3H), 2.39 (s, 3H), 2.36 (s, 3H)	deuterated acetone, 75 MHz: 198.5, 170.0, 141.7, 141.1, 140.6 (t, ² <i>J</i> = 28.5 Hz), 138.9, 133.9 (t, ⁴ <i>J</i> = 27.1 Hz), 132.6, 132.1 (t, ³ <i>J</i> = 7.5 Hz), 131.4, 131.1 (t, ⁴ <i>J</i> = 3.4 Hz), 130.4, 130.0 (t, ³ <i>J</i> = 7.9 Hz), 127.2 (t, ³ <i>J</i> = 5.3 Hz), 122.5 (t, ¹ <i>J</i> = 241.7 Hz), 27.7, 20.8, 20.3	CDCl₃, 282 MHz: – 82.87 (s)	calcd. For C ₁₈ H ₁₆ O ₃ F ₂ Na: m/z [M + Na] ⁺ 341.09597; found: 341.0960 (0 ppm)
A5	CDCl₃, 300 MHz: 7.47 (s, 1H), 7.43 (s, 1H), 7.30 (s, 1H), 7.15–7.17 (m, 3H), 2.81 (sext, 1H, <i>J</i> = 6.9 Hz), 2.27 (s, 3H), 2.24 (s, 3H), 1.14 (d, 6H, <i>J</i> = 6.9 Hz)	CDCl₃, 75 MHz: 172.7, 148.7, 140.5, 138.6, 137.6 (t, ² <i>J</i> = 27.2 Hz), 133.6 (t, ² <i>J</i> = 27.7 Hz), 131.4, 128.8 (t, ³ <i>J</i> = 7.8 Hz), 127.9 (2C), 127.7 (t, ⁴ <i>J</i> = 1.6 Hz), 124.1 (t, ² <i>J</i> = 5.0 Hz), 123.6 (t, ³ <i>J</i> = 5.2 Hz), 120.6 (t, ¹ <i>J</i> = 241.7 Hz), 34.1, 23.8 (2C), 19.9, 19.4	CDCl₃, 282 MHz: – 81.93 (s)	calcd. For C ₁₉ H ₂₀ O ₂ F ₂ Na: m/z [M + Na] ⁺ 341.13236; found: 341.1321 (1 ppm); C ₁₉ H ₁₉ O ₂ FNa: m/z [M-HF + Na] ⁺ 321.12613; found: 321.1260 (0 ppm); C ₁₉ H ₁₉ O ₂ F ₂ Na ₂ : m/z [M-H + 2Na] ⁺ 363.1143; found: 363.1157 (4 ppm); C ₁₉ H ₂₀ O ₂ F ₂ K: m/z [M + K] ⁺ 357.10629; found: 357.1059 (1 ppm); C ₁₉ H ₁₉ O ₂ : m/z [M-HF-F] ⁺ 279.13796; found: 279.1379 (0 ppm)

1EQG) [13] and murine COX-2 (4ph9) [14] complexed with ibuprofen were selected for docking simulations using Autodock Vina (PMID: 19499576) optimized for virtual screening. The numbering of the amino acid residues in the PDB is different between ovine COX-1 and murine COX-2, i.e. Arg120 in COX-1 corresponds to Arg121 in murine COX-2. Water and other heteroatoms were removed from the structure. Chain A was retained including ibuprofen and heme group. Hydrogen atoms were added, atom typing, and partial charges were assigned using Amber forcefield in Chimera (PMID: 15264254). Corresponding ligand-receptor binding energies were estimated in kcal/mol and averaged for best poses that recapitulate ibuprofen binding. A single interacting conformation was retained after visual inspection in Maestro (Schrödinger, LLC).

Data analysis

IL-6, nitrite and PGE₂ measurement were determined from 3 to 5 independent experiments and expressed as percentage of LPS alone and expressed as mean ± SEM. COX-1 activity for the compounds were expressed as percentage of PGE₂ measured in cells exposed to vehicle and AA, and as percentage of PGE₂ in cells treated with LPS, ASA and AA for COX-2. Curve fitting and calculation of the IC₅₀ values were done using Grafit7 Software (Erithacus software, Staines, UK) and GraphPad Prism 6. Images of western blot were analyzed using ImageJ Software (version 1.52a, NIH, MA). Ratio of COX-2 to β-actin was determined and the results are expressed as fold of LPS signal.

Statistical analysis was performed using one-way ANOVA, followed by Dunnett's multiple comparisons test. Differences were considered significant when $p < 0.05$ (GraphPad Prism 6 Software, La Jolla, CA, USA).

Supplementary information

Supplementary information accompanies this paper at <https://doi.org/10.1186/s13065-019-0640-5>.

Additional file 1. Proton (H), carbon (C) and fluorine (F) NMR spectra for intermediates 4 to 18 and for compounds A1 to A5.

Additional file 2. ARRIVE Check list.

Abbreviations

AA: arachidonic acid; ASA: acetylsalicylic acid; BMDM: bone marrow-derived macrophages; COX: cyclooxygenase; FBS: fetal bovine serum; IL-6: interleukin-6; LPS: lipopolysaccharide; NO: nitric oxide; NOS-II: nitric oxide synthase-II; NSAIDs: non-steroidal anti-inflammatory drugs; PGE₂: prostaglandin E₂.

Acknowledgements

We thank the plate-forme of the Centre Régional de Mesures Physiques de l'Ouest (CRMPO) in Rennes, France for the mass spectral analysis. We thank all members the teams (Beirut and Rennes) for their kind help and stimulating discussions.

Authors' contributions

Study concept and design (AH, AHachem and EH); design of the molecules and chemical synthesis (AHachem, LH, RG); acquisition of data (AA, LH, GEA); NH performed the molecular docking; analysis and interpretation of data (AA, LH, SG, GEA, OD, NB, BB, AHachem, EH, AH); IC₅₀ analysis and fitting (OD and AA); drafting of the manuscript (AA, LH, GEA, AHachem, EH, AA); critical revision of the manuscript for important intellectual content (AA, LH, GEA, RG, AHachem, EH, AH); statistical analysis (AA, AH); study supervision (AHachem, EH, AH). AHachem, EH and AH provided financial support. All authors read and approved the final manuscript.

Funding

This work was supported by the Research Grant Program at the Lebanese University, Lebanon (Ali Hachem and Eva Hamade) and the Medical Practice Plan and the University Research Board of the American University of Beirut (Aida Habib) (Grant No. 320024).

Data availability

The data used to support the findings of this study are available from the corresponding author upon request.

Competing interests

The authors declare that they have no competing interests.

Author details

¹ Department of Biochemistry and Molecular Genetics, Faculty of Medicine, American University of Beirut, Beirut, Lebanon. ² Laboratory of Cancer Biology and Molecular Immunology, Faculty of Sciences I, Lebanese University, Hadath, Beirut, Lebanon. ³ Laboratory for Medicinal Chemistry and Natural Products, Faculty of Sciences I and PRAISE-EDST Lebanese University, Beirut, Lebanon. ⁴ Integrative Systems Biology, Institut de Recherches Cliniques de Montréal, Montreal, QC, Canada. ⁵ Department of Biology, Faculty of Sciences II, EDST, Lebanese University, Fanar, Lebanon. ⁶ Université de Rennes, CNRS, ISCR (Institut des Sciences Chimiques de Rennes) UMR 6226, 35000 Rennes, France. ⁷ Université de Paris, Centre de Recherche sur l'Inflammation (CRI), INSERM, UMR1149, CNRS, ERL 8252, 75018 Paris, France. ⁸ Present Address: Department of Electrical and Computer Engineering, American University of Beirut, Beirut, Lebanon.

Received: 12 July 2019 Accepted: 3 October 2019

Published online: 31 October 2019

References

- Özbey F, Taslimi P, Gülçin İ, Maraş A, Göksu S, Supuran CT (2016) Synthesis of diaryl ethers with acetylcholinesterase, butyrylcholinesterase and carbonic anhydrase inhibitory actions. *J Enzyme Inhib Med Chem* 31(sup2):79–85
- Jung N, Bräse S (2009) Synthesis of natural products on solid phases via copper-mediated coupling: synthesis of the aristogin family, spirafornin a, and hernandial. *Eur J Org Chem* 26:4494–4502
- Moore RA, Derry S, McQuay HJ, Wiffen PJ (2011) Single dose oral analgesics for acute postoperative pain in adults. *Cochrane Database of Systematic Reviews* 9:CD008659
- Khanum SA, Begum BA, Girish V, Khanum NF (2010) Synthesis and evaluation of benzophenone-N-ethyl morpholine ethers as anti-inflammatory agents. *Int J Biomed Sci* 6(1):60–65
- Terrazas PM, de Souza Marques E, Mariano LN, Cechinel-Filho V, Niero R, Andrade SF, Maistro EL (2013) Benzophenone guttiferone A from *Garcinia achachairu* Rusby (Clusiaceae) presents genotoxic effects in different cells of mice. *PLoS ONE* 8(11):e76485

6. Deep A, Jain S, Sharma PC (2010) Synthesis and anti-inflammatory activity of some novel biphenyl-4-carboxylic acid 5-(arylidene)-2-(aryl)-4-oxothiazolidin-3-yl amides. *Acta Pol Pharm* 67(1):63–67
7. Thuronyi BW, Chang MC (2015) Synthetic biology approaches to fluorinated polyketides. *Acc Chem Res* 48(3):584–592
8. Muller K, Faeh C, Diederich F (2007) Fluorine in pharmaceuticals: looking beyond intuition. *Science (New York, NY)* 317(5846):1881–1886
9. Shaughnessy MJ, Harsanyi A, Li J, Bright T, Murphy CD, Sandford G (2014) Targeted fluorination of a nonsteroidal anti-inflammatory drug to prolong metabolic half-life. *ChemMedChem* 9(4):733–736
10. Dang H, Whittaker AM, Lalic G (2016) Catalytic activation of a single C-F bond in trifluoromethyl arenes. *Chem Sci* 7(1):505–509
11. Gillis EP, Eastman KJ, Hill MD, Donnelly DJ, Meanwell NA (2015) Applications of fluorine in medicinal chemistry. *J Med Chem* 58(21):8315–8359
12. Khalaf A, Grée D, Abdallah H, Jaber N, Hachem A, Grée R (2011) A new flexible strategy for the synthesis of gem-difluoro-bisarylic derivatives and heterocyclic analogues. *Tetrahedron* 67(21):3881–3886
13. Selinsky BS, Gupta K, Sharkey CT, Loll PJ (2001) Structural analysis of NSAID binding by prostaglandin H2 synthase: time-dependent and time-independent inhibitors elicit identical enzyme conformations. *Biochemistry* 40(17):5172–5180
14. Orlando BJ, Lucido MJ, Malkowski MG (2015) The structure of ibuprofen bound to cyclooxygenase-2. *J Struct Biol* 189(1):62–66
15. Hariss L, Ibrahim R, Jaber N, Roisnel T, Grée R, Hachem A (2018) A general approach to various five- and six-membered gem-difluoroheterocycles: application to the synthesis of fluorinated analogues of sedamine. *Eur J Org Chem* 2018(27–28):3782–3791
16. Habib A, Chokr D, Wan J, Hegde P, Mabire M, Siebert M, Ribeiro-Parenti L, Le Gall M, Letteron P, Pilard N et al (2019) Inhibition of monoacylglycerol lipase, an anti-inflammatory and antifibrogenic strategy in the liver. *Gut* 68:522–532
17. El-Achkar GA, Jouni M, Mrad MF, Hirz T, El Hachem N, Khalaf A, Hammoud S, Fayyad-Kazan H, Eid AA, Badran B et al (2015) Thiazole derivatives as inhibitors of cyclooxygenases in vitro and in vivo. *Eur J Pharmacol* 750:66–73
18. Habib A, Shamseddeen I, Nasrallah MS, Antoun TA, Nemer G, Bertoglio J, Badreddine R, Badr KF (2007) Modulation of COX-2 expression by statins in human monocytic cells. *FASEB J* 21(8):1665–1674
19. Mouawad CA, Mrad MF, Al-Hariri M, Soussi H, Hamade E, Alam J, Habib A (2013) Role of nitric oxide and CCAAT/enhancer-binding protein transcription factor in statin-dependent induction of heme oxygenase-1 in mouse macrophages. *PLoS ONE* 8(5):e64092
20. Creminon C, Frobert Y, Habib A, Maclouf J, Pradelles P, Grassi J (1995) Immunological studies of human constitutive cyclooxygenase (COX-1) using enzyme immunometric assay. *Biochimica Biophysica Acta* 1254(3):333–340
21. Habib A, Bernard C, Lebret M, Creminon C, Esposito B, Tedgui A, Maclouf J (1997) Regulation of the expression of cyclooxygenase-2 by nitric oxide in rat peritoneal macrophages. *J Immunol* 158(8):3845–3851

Publisher's Note

Springer Nature remains neutral with regard to jurisdictional claims in published maps and institutional affiliations.

Ready to submit your research? Choose BMC and benefit from:

- fast, convenient online submission
- thorough peer review by experienced researchers in your field
- rapid publication on acceptance
- support for research data, including large and complex data types
- gold Open Access which fosters wider collaboration and increased citations
- maximum visibility for your research: over 100M website views per year

At BMC, research is always in progress.

Learn more biomedcentral.com/submissions

